Renormalization of the electron-spin-fluctuation interaction in the $t - t' - U$ Hubbard model

Z. B. Huang[1,2], W. Hanke[1], E. Arrigoni[3], and A. V. Chubukov[4]

[1]*Institut für Theoretische Physik, Universität Würzburg, am Hubland, 97074 Würzburg, Germany*
[2]*Department of Physics, Hubei University, Wuhan 430062, PRC*
[3]*Institut für Theoretische Physik, Technische Universität Graz, Petersgasse 16, A-8010 Graz, Austria and*
[4]*Department of Physics, University of Wisconsin, Madison, Wisconsin 53706, USA*
(Dated: February 6, 2008)

We study the renormalization of the electron-spin-fluctuation (el-sp) vertex in a two-dimensional Hubbard model with nearest-neighbor (t) and next-nearest-neighbor (t') hopping by a Quantum-Monte-Carlo calculation. We distinguish between el-sp vertices involving interacting particles and quasiparticles, i.e. separate the renormalizations of the vertex from that of the quasiparticle residue $1/Z$. We show that for $t' = 0$, the renormalized el-sp vertex, not dressed by $1/Z$, decreases with decreasing temperature at all momentum transfers. As a consequence, the effective pairing interaction mediated by antiferromagnetic spin fluctuations is reduced due to vertex corrections. The inclusion of a finite $t'/t < 0$, increases the Landau damping rate of spin fluctuations, especially in the overdoped region. The increased damping rate leads to smaller vertex corrections, in agreement with earlier diagrammatic calculations. Still, corrections reduce the spin-fermion vertex even at finite t'.

I. INTRODUCTION

The nature of the spin-fluctuation mediated interaction between charge carriers continues to attract high interest in the high-T_c superconductivity research[1,2,3,4,5,6]. Theoretical calculations for the doped Hubbard and $t − J$ models suggest that the strongest interaction between fermions is due to antiferromagnetic (AF) spin fluctuations. The low-energy description of this interaction has been advanced in the framework of the spin-fermion model[6]. A magnetically mediated interaction has been intensively studied since the early days of high-T_c era because AF spin fluctuations induce $d−$wave pairing between fermions[1]. Various numerical and analytical calculations based on Hubbard and $t − J$ models, as well as semi-phenomenological spin-fermion models, have been performed in the normal and superconducting states of the cuprates. The results of these calculations are in quite good agreement with a large number of experimental data. In particular, these calculations show that the magnetic response in a $d−$wave superconducting state contains a resonance peak, in addition to a gapped continuum. The location of the peak, and its "negative" dispersion are in agreement with experimental data. It has been argued[8] that the scattering from the resonance is strong enough to explain the peak-dip-hump feature in the fermionic spectral function, the $S−$shape dispersion for antinodal fermions, and similar features in SIS tunneling, optical conductivity, and Raman response.

The strength of the feedback effects from the resonance peak on fermions, and the magnitude of the spin-mediated T_c depend on the size of the spin-fermion coupling. The estimates for the coupling strength still vary substantially. Abanov et al argued[7] that the coupling g is comparable to the Hubbard U and is quite strong, $g \sim 0.7eV$. On the other hand, Kee *et al.*[9] argued that the effective spin-fermion coupling is much weaker

$g \sim 0.014eV$. In the latter work[9], the coupling was extracted from the specific heat data. To a large extent, the difference between the two results is related to different choices for the fermionic density of states N_0: a large value of g is obtained by assuming a large Luttinger Fermi surface, with $N_0 \sim 1eV^{-1}$ (Ref. 7), while a smaller g is obtained by assuming that the density of states $N_0 \sim J^{-1} \sim 10eV^{-1}$ is the same as in a weakly doped quantum AF.

This difference brings in the issue of how much the full spin-fermion vertex $g_{\mathbf{kq}}$ differs from the bare $g^0_{\mathbf{kq}}$ due to vertex corrections. Here, $\mathbf{k}$ and $\mathbf{k} + \mathbf{q}$ are incoming and outgoing fermionic momenta, and $\mathbf{q}$ is the bosonic momentum. The ratio $\Gamma(\mathbf{k}, \mathbf{q}) = g_{\mathbf{kq}}/g^0_{\mathbf{kq}}$ determines the vertex renormalization originating from electronic correlations. Some of us have recently shown numerically that this quantity is substantially renormalized by strong electronic correlations both for the electron-phonon (el-ph) vertex[10] as well as for the el-sp vertex[11].

Within the spin-fermion model, the role of the vertex renormalization is well understood in the limits of very small and relatively large doping. At very small doping x, when long-range AF order is still present, nearly all carriers are localized, and doped fermions form small pockets around $(\pi/2, \pi/2)$ and symmetry related points. In this situation, the full spin-fermion vertex $g_{\mathbf{kq}}$ vanishes when $\mathbf{q}$ coincides with the antiferromagnetic momentum $\mathbf{Q} \equiv (\pi, \pi)$. The vanishing of $g_{\mathbf{kQ}}$ is the consequence of the Adler principle that the interaction should preserve massless Goldstone bosons in the theory and, therefore, should vanish at the ordering momentum of Goldstone bosons. For $\mathbf{q} \neq \mathbf{Q}$, the vertex is non-zero, but small in $|\mathbf{q} - \mathbf{Q}|/|\mathbf{Q}|$. Mathematically, the vanishing of $g_{\mathbf{kQ}}$ is the result of dressing up of the bare interaction $g^0_{\mathbf{kQ}}$ by coherence factors, associated with the antiferromagnetic order. From this perspective, the strong reduction of $g_{\mathbf{kq}}$ when $\mathbf{q}$ is close to $\mathbf{Q}$ is the result of a strong vertex renor-

malization. Schrieffer argued[12] that, if the pocket-like Fermi surface survives even when long-range AF order is lost, the strong vertex renormalization extends into the paramagnetic phase. According to Ref. 12

$$\Gamma^2(\mathbf{k}, \mathbf{q}) \propto [(\mathbf{q} - \mathbf{Q})^2 + \frac{1}{\xi^2}] \sim \frac{1}{[\chi(\mathbf{q}, \omega = 0)]}, \quad (1)$$

where ξ is the AF correlation length. Once Eq. (1) is valid, the effective spin-mediated interaction

$$V(\mathbf{k}, \mathbf{q}) \propto |\Gamma(\mathbf{k}, \mathbf{q})|^2 \chi(\mathbf{q}), \quad (2)$$

is considerably weaker than without vertex renormalization, and, most importantly, it is no longer peaked at $\mathbf{q} \sim \mathbf{Q}$. This is an important fact, since the peak structure at $\mathbf{q} \sim \mathbf{Q}$ was responsible for a strong attractive $d-$wave component in the pairing potential. The magnetically-mediated $d-$wave pairing is still possible even in this situation, but the corresponding T_c is much smaller than one would get without vertex corrections[13].

In the opposite limit of large doping, fermions are itinerant, and have a large Fermi surface which crosses the magnetic Brillouin zone boundary at hot spots (this requires a sufficiently strong next-nearest-neighbor hopping). A spin-fluctuation with momentum near $\mathbf{Q}$ then can decay into a particle and a hole. Analytical calculations within the spin-fermion model show that in this situation, the vertex is only weakly renormalized, and actually increases with respect to its bare value, i. e. $g_{\mathbf{kQ}} > g^0_{\mathbf{kQ}}$[6,14]. More precisely, the relation between $g_{\mathbf{kQ}}$ and $g^0_{\mathbf{kQ}}$ depends on the angle $\phi \leq \pi$ between Fermi velocities at hot spots separated by $\mathbf{Q}$[6]:

$$\Gamma(k, Q) = \frac{g_{\mathbf{kQ}}}{g^0_{\mathbf{kQ}}} = \left(1 + \frac{\phi}{4\pi} \log \xi/\xi_0\right), \quad (3)$$

where ξ_0 is of order 1. Equation (3) shows that the renormalization is largest when $\phi \to \pi$. This limit corresponds to an almost nested Fermi surface at hot spots. In optimally doped cuprates, the velocities at the hot spots separated by $\mathbf{Q}$ are almost perpendicular to each other, i. e., $\phi \approx \pi/2$. For $\xi \sim 2$, the vertex correction is then about 10% (even smaller, $\sim 4\%$, when one adds regular terms[15,16]).

The difference between the itinerant and localized limits raises the question how vertex corrections evolve as the system approaches half-filling. One attempt to address this issue was undertaken in Ref. 16. The authors of Ref. 16 considered a toy spin-fermion model in which one can study the evolution from the Luttinger Fermi surface towards hole pockets. This evolution involves a topological transition below which a pocket is splitted from a large Fermi surface, and the Luttinger theorem breaks down. Within this model, vertex corrections evolve together with the Fermi surface: they are small and positive (i. e. $g_{\mathbf{kQ}} > g^0_{\mathbf{kQ}}$) in the limit when the Fermi surface is large, but change their sign near the topological transition, become negative and rapidly increase in magnitude

as the Fermi surface evolves towards hole pockets. For a pocket-like Fermi surface, vertex corrections almost cancel the bare vertex, and the full $g_{\mathbf{kq}}$ coincides with Schrieffer's result, Eq. (1).

In this paper, we address the issue of the strength of vertex corrections in the two-dimensional $t - t' - U$ Hubbard model by means of a quite accurate numerical method – the determinantal Monte-Carlo[17] algorithm. The purpose of our calculation is to explore the extent of validity in doping and temperature of Schrieffer's argument[12] as well as of the spin-fermion model calculation[6]: Whereas the analytical results are only valid when the correlation length ξ is large, Monte-Carlo calculations are not restricted by this condition. We also want to get an insight as up to what extent a description in terms of low-energy spin degrees of freedom, i. e. in terms of a spin-fermion model is appropriate for the Hubbard model.

Vertex corrections have been analyzed by some of us in Ref. 11. The present paper extends this earlier letter in three different directions. First, in order to separate vertex and quasiparticle renormalization effects, we analyze the vertex renormalization and the pairing interaction with and without the inclusion of the wave-function renormalization Z. The vertex without the renormalization of Z is labeled by $\Gamma(p, q)$ before and in Eq. (7) below. This vertex is for the interaction between spin fluctuations and strongly interacting particles. This vertex has to be used for comparison with analytical results which don't include the rescaling by the fermionic Z. The fully renormalized vertex is the one rescaled by Z (we label it by $\gamma(p, q)$, see Eq. (9) below)[18]. It describes the interaction between spin fluctuations and quasiparticles. We discuss the difference between the two vertices in Sec. III, and also discuss there the behavior of the pairing interaction between interacting particles and quasiparticles. Second, we calculate the momentum dependence of the vertex. Third, we discuss in detail the effect of bosonic damping on the strength of the vertex renormalization. We show that the introduction of a next-nearest-neighbor hopping t', which makes the bosonic damping possible, substantially reduces the renormalization of Γ (but not of γ).

Our numerical Monte Carlo simulations are performed on a 8×8 lattice at different doping densities and different temperatures. In our finite lattice, the $(\pi, 0)$ point is the one closest to the hot spots, so that charge carriers near the $(\pi, 0)$ region are strongly affected by antiferromagnetic spin fluctuations. Therefore, we will mainly concentrate on the particular scattering process in which the incoming electron and spin fluctuation carry momenta $\mathbf{p} = (-\pi, 0)$ and $\mathbf{q} = (\pi, \pi)$, respectively. Within our $\mathbf{p}$-points mesh, the points $\mathbf{p}$ and $\mathbf{p} + \mathbf{q}$ lie sufficiently close to the Fermi surface.

Our paper is organized as follows: In Section II, we define the Hamiltonian and describe the numerical approach, which is based on the Quantum-Monte-Carlo evaluation of the linear response to an external spin per-

turbation. In Section III, we present our numerical results and discuss their qualitative relation with the spin-fermion-model calculation and Eq. 1. Finally, in Section IV, we discuss in detail our main conclusions.

II. MODEL AND NUMERICAL APPROACH

Our starting point is the one-band Hubbard model,

$$
H = -t \sum_{\langle ij \rangle, \sigma} (c_{i\sigma}^\dagger c_{j\sigma} + c_{j\sigma}^\dagger c_{i\sigma}) - t' \sum_{\langle\langle ij \rangle\rangle, \sigma} (c_{i\sigma}^\dagger c_{j\sigma} + c_{j\sigma}^\dagger c_{i\sigma})
$$
$$
+ U \sum_i n_{i\uparrow} n_{i\downarrow}, \tag{4}
$$

Here, the operators $c_{i\sigma}^\dagger$ and $c_{i\sigma}$ as usual create and destroy an electron with spin σ at site i, respectively, and $\langle ij \rangle$ and $\langle\langle ij \rangle\rangle$ denote a sum over nearest and next-nearest neighbor lattice sites i and j, respectively. $n_{i\sigma} = c_{i\sigma}^\dagger c_{i\sigma}$ is the number operator. Finally, U is the onsite Coulomb interaction and the nearest-neighbor hopping t is chosen as the unit of energy. In order to consider the effects of damping, we include a next-nearest-neighbor hopping term t'.

In our simulation, we use a linear-response approach (see also Ref. 10) in order to extract the el-sp vertex. In this method, one formally adds to Eq. (4) the interaction with a momentum- and (imaginary) time-dependent spin-fluctuation field in the z-direction $S_{\mathbf{q}} e^{-iq_0\tau}$[19] in the form[19]

$$
H_{\text{el-sp}} = \sum_{\mathbf{k q} \sigma} g_{\mathbf{k q}}^0 \sigma c_{\mathbf{k+q}\sigma}^\dagger c_{\mathbf{k}\sigma} \; S_{\mathbf{q}} \; e^{-iq_0\tau} , \tag{5}
$$

where $g_{\mathbf{k q}}^0$ is the bare el-sp coupling (equal to the Hubbard U in the one-band Hubbard model). One then considers the "anomalous" single-particle propagator in the presence of this perturbation defined as[19]

$$
G_A(p,q) \equiv -\int_0^\beta d\tau \; e^{i(p_0+q_0)\tau} \langle T_\tau c_{\mathbf{p+q}\sigma}(\tau) c_{\mathbf{p}\sigma}^\dagger(0) \rangle_{H+H_{\text{el-sp}}}, \tag{6}
$$

Here $\langle \rangle_{H+H_{\text{el-sp}}}$ is the Green's function evaluated with the Hamiltonian $H + H_{\text{el-sp}}$. Diagrammatically, $G_A(p,q)$ has the structure shown in Fig. 1, so that the el-sp vertex $\Gamma(p,q)$ can be expressed quite generally in terms of G_A and of the single-particle Green's function $G(p)$ in the form

$$
\Gamma(p,q) = \lim_{S_{\mathbf{q}} \to 0} \frac{1}{g_{kq}^0} \frac{1}{S_{\mathbf{q}}} \frac{1}{1 + U \chi_{zz}(q)} \frac{G_A(p,q)}{G(p+q)G(p)} , \tag{7}
$$

with $\chi_{zz}(q)$ the longitudinal spin susceptibility. Because only the limit $S_{\mathbf{q}} \to 0$ is relevant in Eq. 7, it is sufficient to calculate the leading linear response of G_A to $H_{\text{el-sp}}$, which is given by

$$
G_A(p,q) = S_{\mathbf{q}} \int_0^\beta d\tau e^{i(p_0+q_0)\tau} \int_0^\beta d\tau' e^{-iq_0\tau'} \sum_{\mathbf{k}\sigma'} g_{\mathbf{k q}}^0 \times
$$
$$
\langle T_\tau \sigma' c_{\mathbf{k+q}\sigma'}^\dagger(\tau'+0^+) c_{\mathbf{k}\sigma'}(\tau') c_{\mathbf{p+q}\sigma}(\tau) c_{\mathbf{p}\sigma}^\dagger(0) \rangle_H, \tag{8}
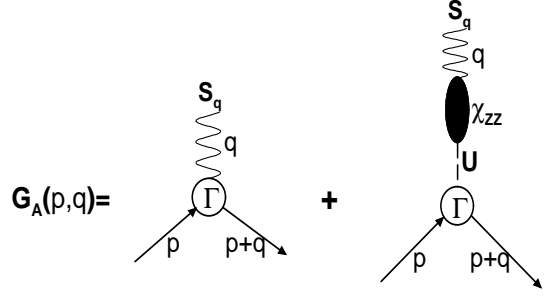$$

FIG. 1: Diagrammatic representation of $G_A(p,q)$ within linear response to $S_{\mathbf{q}}$. The thick solid lines represent dressed single-particle Green's functions of the Hubbard model. The wavy line denotes the external perturbation in Eq. (5). The dashed line represent the Hubbard interaction U and the black ellipse stands for the longitudinal spin susceptibility $\chi_{zz}(q)$.

where 0^+ is a positive infinitesimal. Notice that $S_{\mathbf{q}}$ cancels in Eq. 7. The two-particle Green's function in Eq. (8) is evaluated with respect to the pure Hubbard Hamiltonian (Eq. (4)).

Within a quasiparticle approach, one can shift the wave-function renormalization factor $Z(p) > 1$ from the Green's function into the definition of the effective el-sp vertex.[10] Thus, for states close to the Fermi energy with a single-particle Green's function of the form $G(p) = Z(p)^{-1} (i \, p_0 - E_p)^{-1}$, where E_p is the quasiparticle energy, the effective quasiparticle-spin coupling is given by:

$$
\gamma(p,q) = \frac{\Gamma(p,q)}{\sqrt{Z(p) \, Z(p+q)}} . \tag{9}
$$

Numerically, $Z(p)$ is evaluated as $Z(p) = \text{Im}[1/G(p)]/p_0$[10,19]. Therefore, γ is the vertex between *quasiparticles* and spin fluctuations.

The total pairing interaction V_p for the exchange of a single spin fluctuation can be expressed in terms of the vertex Γ as

$$
V_p(p,q) = |\Gamma(p,q)|^2 \cdot U^2 \cdot \chi_{zz}(q) , \tag{10}
$$

where $\chi_{zz}(q)$ is the spin susceptibility

$$
\chi_{zz}(q) = \frac{1}{2} \int_0^\beta d\tau \; e^{-i \, q_0 \tau} \; \langle T_\tau m_{\mathbf{q}}^z(\tau) m_{-\mathbf{q}}^z(0) \rangle ,
$$

and

$$
m_{\mathbf{q}}^z = \frac{1}{\sqrt{N}} \sum_{\mathbf{k}\sigma} \sigma c_{\mathbf{k+q}\sigma}^\dagger c_{\mathbf{k}\sigma} . \tag{11}
$$

Eq. 10 describes the effective pairing interaction between *interacting particles*. Including the wave-function renormalization as in Eq. 9, we introduce the effective pairing interaction *between quasiparticles* (this is in complete analogy to the treatment of the strong-coupling superconductors in Ref.[20])

$$
v_p(p,q) = \frac{V_p(p,q)}{Z(p) \, Z(p+q)} = |\gamma(p,q)|^2 U^2 \chi_{zz}(q) . \tag{12}
$$

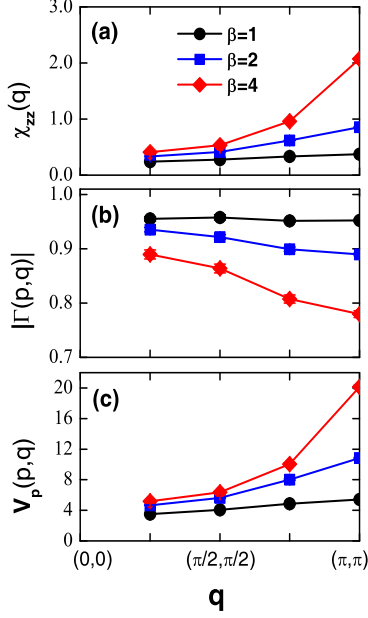FIG. 2: (color online) (a) Spin susceptibility $\chi_{zz}(q)$, (b) the renormalized el-sp vertex $|\Gamma(p,q)|$, and (c) the total pairing interaction $V_p(p,q)$ as a function of spin-fluctuation momentum transfer $\mathbf{q}$. Here $U = 4$, $t' = 0$, $\mathbf{p} = (-\pi, 0)$, and the doping density $\delta = 0.12$. The value of the inverse temperature β is indicated by the shape of the symbol.

III. RESULTS AND DISCUSSIONS

In order to explore the momentum structure of the el-sp interaction, we first plot $\chi_{zz}(q)$, $|\Gamma(p,q)|$, and $V_p(p,q)$ versus $\mathbf{q}$ at different temperatures in Fig. 2. Here, the spin-fluctuation momentum transfer $\mathbf{q}$ is along the $(1,1)$ direction and U is at an intermediate coupling value, i.e. $U = 4$. One can readily see that both $\chi_{zz}(q)$ and $V_p(p,q)$ are peaked at momentum transfers around the antiferromagnetic vector $\mathbf{Q} = (\pi, \pi)$, and the strength of the peaks increases when the temperature is lowered. This demonstrates that the $\mathbf{q}$- and T-dependences of the spin susceptibility χ dominate the temperature behavior of the pairing interaction, despite the reduction of the vertex Γ as the temperature is decreased. From Fig. 2, we observe that the decrease with temperature of Γ at large momentum transfers is stronger than at small momentum transfers, indicating that the vertex correction at $\mathbf{q} \sim \mathbf{Q}$
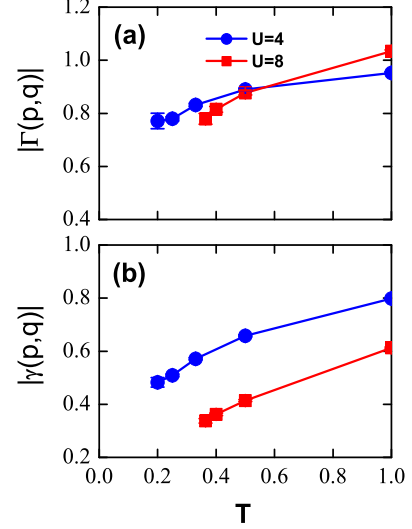
Clearly, both $V_p(p,q)$ and $v_p(p,q)$ contain the contributions from both the real and imaginary parts of the vertex. Within a Quantum-Monte-Carlo approach, the effects and strength of the particle-particle vertex in a given channel can be also indirectly measured by comparing the full pairing susceptibility with the corresponding "bubble" approximation[21].

FIG. 3: (color online) The absolute values of the (complex) renormalized el-sp vertices $|\Gamma(p,q)|$ and $|\gamma(p,q)|$ vs T at $U = 4$ and $U = 8$ at the doping density $\delta = 0.12$. We set $\mathbf{p} = (-\pi, 0)$, $\mathbf{q} = (\pi, \pi)$, and $t' = 0$.

is larger than at small $\mathbf{q}$. This $\mathbf{q}$-dependence of the el-sp vertex is qualitatively in agreement with the prediction of Eq.(1). Our finding is also in good agreement with the work of Bulut et al.[22] (carried out at $U = 4$), which shows a value of $g = 0.8$ (corresponding $|\Gamma| = 0.8$ in our notation) can produce an effective coupling gU which is consistent with the results of Monte Carlo calculation of the irreducible particle-hole vertex, and that the effective particle-particle interaction originating from the Hubbard U increases with lowering temperature and can reach large values.

Monte Carlo results for $\Gamma(p,q)$, $\gamma(p,q)$, $Z(p)$, $V_p(p,q)$ and $v_p(p,q)$ are displayed in Figs. 3 and 4 for intermediate as well as strong correlation. We compute the vertices at zero bosonic Matsubara frequency and the smallest fermionic Matsubara frequency $\omega_1 = \pi T$. Because ω_1 is finite, and also because at a nonzero doping, the excitation spectrum is particle-hole asymmetric, the vertices Γ and γ have both real and imaginary parts (the imaginary part obviously vanishes at $T = 0$). We notice that in the underdoped regime ($\delta = 0.12$) for both intermediate ($U = 4$) and strong correlation ($U = 8$), both $|\Gamma|$ and $|\gamma|$ are strongly renormalized below a characteristic temperature ($T \lesssim J = 0.5$ for $U = 8$). Although our simulation cannot reach low temperatures, a clear trend is observable in both $|\Gamma|$ and $|\gamma|$, which tend to go to small values at low temperatures, at least for $U = 8$. A more careful look shows that the reduction of the vertices Γ and γ is chiefly due to the reduction of $Re\Gamma$ and $Re\gamma$. The imaginary parts of the vertices are small at weak and intermediate correlations (at our lowest accessible T), but for $U = 8$ they can become comparable to
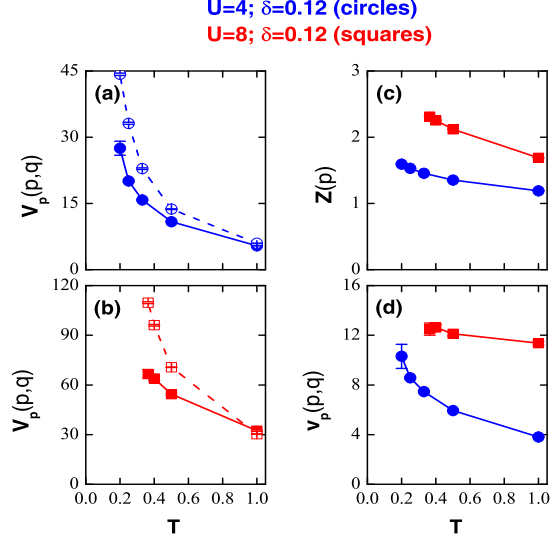
FIG. 4: (color online) The pairing interaction $V_p(p,q)$ vs T for (a) $U = 4$ and (b) $U = 8$ at the doping density $\delta = 0.12$ (full symbols, the solid line is a guide to the eye). The open symbols (dashed line) show the RPA results. In panel (c), we show the T-dependence of the wave-function renormalization $Z(p)$ and in panel (d) the effective pairing interactions $v_p(p,q)$ between quasiparticles. In all panels, $\mathbf{p} = (-\pi, 0)$, $\mathbf{q} = (\pi, \pi)$, and $t' = 0$.

the real parts.

Further, our numerical results presented in Fig. 4 clearly show that, in both intermediate- and strong-correlation regimes, the renormalized pairing interaction V_p (which does not include the dressing by the quasiparticle Z) is smaller than the RPA result obtained with the full susceptibility χ_{zz}. The difference becomes strongest at the lowest accessible temperatures. The qualitative temperature behavior of the effective pairing interaction between quasiparticles v_p, is quite similar to V_p in the intermediate-correlation ($U = 4$) regime. However, it is quite different in the strong-correlation ($U = 8$) regime, where it displays a mild increase or a saturation at low T's. Based on the results shown in Fig. 4, we conclude that for $t' = 0$, both vertex corrections and the renormalization of Z are important for the spin-mediated pairing interaction. Vertex corrections suppress $V_p(p,q)$ compared to the case of free fermions. The rescaling by Z further suppresses the effective pairing interaction between quasiparticles, $v_p(p,q)$. Note, though, that the pairing interaction $V_p(p,q)$ at a bosonic $q = (\pi, \pi)$ and fermionic p near the antinodal point still increases with decreasing temperature.

Fig. 4 shows that vertex corrections are substantial even in the case when the AF correlation length ξ is quite small[23]. i. e. of order of the Cu-Cu distance. This is in contrast to the situation discussed by Schrieffer in which holes move in an AF background, which is unaffected by
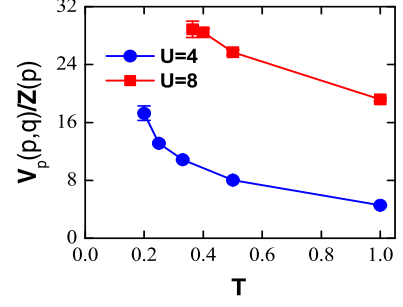

FIG. 5: (color online) $V_p(p,q)/Z(p)$ vs T for $U = 4$ and $U = 8$ at the doping density $\delta = 0.12$ (full symbols, the solid line is a guide to the eye). $\mathbf{p}$ and $\mathbf{q}$ are the same as in Fig. 4.

the charge carriers, i. e. ξ is large. How can we understand this result? In the AF precursor (large-ξ) case[12,16], the vanishing of the el-sp interaction in the long-range ordered AF state is the result of dressing up of the bare interaction by the AF coherence factor, which is small at the top of the valence band. The coherence factor is due to the interference effect of the quasiparticle, which forms a "spin-bag", i. e. a hole dressed by a short-range AF background. Although in our calculation the AF precursor is no longer present, it is well established from our earlier QMC work on the evolution of the single-particle spectral function $A(\mathbf{k}, \omega)$[23] from an insulator to a metal that below $T \sim J$, the electronic excitations display an essentially doping-independent feature. More precisely, a "band" of width J forms, in which "spin-bag"-like quasiparticles propagate coherently. The continuous evolution can be traced back to one and the same many-body origin: the doping-dependent AF spin-spin correlation. Therefore, we argue that the interference effect of the spin-bag quasiparticle plays a similar role in reducing the el-sp vertex in the strongly-correlated underdoped regime.

Above we considered the pairing vertices for interacting particles and for quasiparticles. The actual strength of the pairing interaction is proportional to the product of the effective interaction v_p and the density of states at the Fermi level $N(E_F)$. Since we restricted with only the pole component of G, the conservation of the particle number implies that $N(E_F)$ is increased by a factor Z with respect to the noninteracting density of states $N_0(E_F)$, i.e., $N(E_F)v_p = N_0(E_F) V_p/Z$. This is similar to the case of the electron-phonon mediated pairing, where the interaction is also rescaled by one power of Z (this last rescaling is a well-known McMillan result $\lambda \rightarrow \lambda/(1+\lambda)$. Our consideration, in which we defined Z as the overall wave-function renormalization is formally different from electron-phonon problem, where the fermionic self-energy depends only on frequency. However, the final result is the same as in the case where self-energy only depends on frequency, the density of states is not renormalized
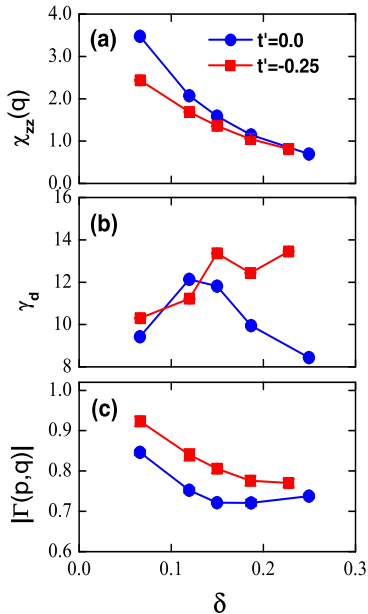
FIG. 6: (color online) (a) Spin susceptibility $\chi_{zz}(q)$, (b) "damping rate" γ_d, and (c) el-sp vertex $|\Gamma(p,q)|$ as a function of doping density δ for $U = 4$. The value of t' is indicated by the shape of the symbol. Here $\mathbf{p} = (-\pi, 0)$, $\mathbf{q} = (\pi, \pi)$, and $\beta = 4$.

FIG. 7: (color online) (a) El-sp vertex $|\gamma(p,q)|$ and (b) $V_p(p,q)/Z(p)$ as a function of doping density δ for $U = 4$. $\mathbf{p}$ and $\mathbf{q}$ are the same as in Fig. 6.

by Z, but one power of Z, compared to $v_p \sim V_p/Z^2$ is eliminated by the mass renormalization $m^*/m = Z$.

In order to have a measure of the pairing strength including the renormalization of the density of states, we thus plot the quantity $V_p(p,q)/Z(p)$ in Fig. 5 as a function of temperature for $\delta = 0.12$. We observe that $V_p(p,q)/Z(p)$ increases with decreasing temperature in both intermediate- and strong-correlation regimes. On the other hand, the suppression of V_p due to vertex corrections and the increase of Z with decreasing temperature considerably reduce the pairing (i. e., without vertex corrections), in particular in the low-temperature regime.

As discussed in the Introduction, previous work on the spin-fermion model[6] suggests that the vertex correction $|\Gamma - 1|$ (not including Z) gets considerably reduced, whenever spin fluctuations get damped. To explore this fact, we have compared numerical results for different values of the next-nearest-neighbor hopping ($t' = 0$ and $t' = -0.25$), since one expects the damping to increase for larger negative t'. The spin susceptibility χ_{zz}, a quantity proportional to the damping rate γ_d, and the el-sp vertex Γ are plotted in Figs. 6(a)-6(c) as a function of doping density. When $t' = 0$, the Fermi surface is particlelike and encloses the zone center $\Gamma = (0, 0)$. On the other hand, when $t' = -0.25$, the Fermi surface is holelike and encloses the zone corner $Q = (\pi, \pi)$, and, in particular, it crosses the magnetic Brillouin Zone boundary at so-called hot spots. In this second case, spin fluctu-
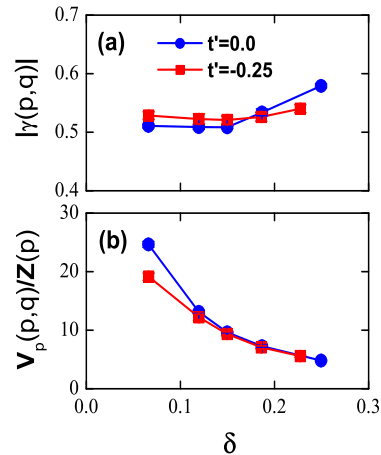
ations get strongly damped due to the decay into particle and holes near the Fermi surface. Due to the finite temperature and short correlation length, a damping of spin fluctuations is also present for $t' = 0$. The quantity $\gamma_d = b/c$ shown in Fig. 6, is obtained by fitting the spin susceptibility $\chi(q, i\omega_m)^{-1}$ to the form $a + b\omega_m + c\omega_m^2$, and is, thus, proportional to the spin damping rate. In the underdoped region, the spin susceptibility is strongly suppressed by a negative t' due to its frustrating effect on the AF alignment, whereas the difference of γ_d is small, as seen in Fig. 6(a) and Fig. 6(b). On the other hand, in the overdoped region, where the holelike Fermi surface passes close to $(\pi, 0)$ and symmetry points (whereas the particlelike Fermi surface moves away from the magnetic Brillouin zone boundary), t' has little effect on the spin susceptibility, while the spin damping rate is dramatically increased by a negative t'. Fig. 6(c) clearly shows that the el-sp vertex $|\Gamma|$ is larger for $t' = -0.25$ than for $t' = 0$, demonstrating that the vertex correction is reduced either by suppressing the spin susceptibility or by increasing the spin damping rate. However, the largest difference in $|\Gamma|$ is not observed at the smallest doping density $\delta = 0.066$, where the suppression of the spin susceptibility is strongest, or near the doping density $\delta = 0.20$, where the difference of the damping rates is largest. This result suggests that, although both the spin susceptibility and the damping of spin fluctuations are related to the magnitude of vertex corrections, they are probably not the only relevant factors.

In Figs. 7(a) and 7(b) we show the effects of the next-nearest-neighbor hopping t' on the effective el-sp vertex $\gamma(p,q)$ and the effective pairing interaction $V_p(p,q)/Z(p)$. In contrast to Γ, the vertex $\gamma \sim \Gamma/Z$ shows a weak dependence on t' (and also on δ), and in the overdoped regime is even smaller for $t' = -0.25$ than for $t' = 0$. The differ-

ent behavior of the vertices Γ and γ is obviously due to the Z factor, which increases with increasing $|t'|$ and/or decreasing doping. The result fo $V_p(p,q)/Z(p)$ shows that the pairing strength has almost no dependence on t' in the optimal and overdoped regimes, and is somewhat reduced at a negative t' in the underdoped regime.

Finally, we comment on the overall sign of the vertex correction. In our cases studied, as shown in Fig. 2 and Fig. 6, $|\Gamma|$ is always less than 1, indicating that the el-sp interaction is suppressed by vertex corrections. This is in contrast to the finding in the spin-fermion model, which shows that the total vertex correction at moderate doping has a positive sign, i. e., vertex correction actually increases the el-sp interaction. This effect, however, is rather small and for moderate ξ may be overshadowed by the contributions from high-energies ($O(E_F)$), not included in the low-energy spin-fermion models. The comparison between our calculations and the results in the spin-fermion model shows that, while the effect of damping of spin fluctuations on vertex corrections is quite robust and agrees with low-energy considerations, the sign and the magnitude of the vertex correction near optimal doping may be model dependent.

IV. CONCLUSIONS

In summary, based on Quantum-Monte-Carlo simulations, we have studied the renormalization of the el-sp vertex in the two-dimensional $t - t' - U$ Hubbard model. We found that the fully renormalized el-sp vertex between bosons and free fermions decreases quite generally with decreasing temperature at all spin-fluctuation momentum transfers. We distinguished between vertex renormalization itself and the renormalization due to the dressing of the vertex by quasiparticle Z factors. We analyzed the effect of adding a negative next-nearest-neighbor hopping term t' to the dispersion. This term changes the topology of the Fermi surface and allows a spin fluctuations to decay into an electron-hole pair. We found that t' reduces vertex corrections (but not Z), in agreement with previous results on the spin-fermion model. However, in contrast to Ref. 6, we did not observe a positive vertex correction, i. e. the renormalized vertex is always smaller than the bare one.

The suppression of the fully renormalized el-sp vertex, particularly at $t' = 0$, gives rise to a substantial reduction of the pairing mediated by antiferromagnetic spin fluctuations in both the intermediate- and strong-correlation regimes. This result extends Schrieffer's argument (Eq. 1) about the suppression of the el-sp vertex to the case in which the AF precursor is no longer present. Notice, however, that Γ and χ behave in the opposite way (as implied by Eq. 1, only when one considers their *temperature* behavior. In contrast, when *doping* decreases at a fixed temperature, Γ increases with increasing χ (the results are not shown here). Thus, in the situation when the system is away from the AF precursor, there is no general proportionality relation implied in Eq. 1.

[1] D.J. Scalapino, Physics Reports **250**, 329-365 (1995).

[2] M. Imada, A. Fujimori, and Y. Tokura, Rev. Mod. Phys. **70**, 1039 (1998).

[3] F. Assaad, W. Hanke, and D. J. Scalapino, Phys. Rev. Lett. **71**, 1915 (1993), and Phys. Rev. B **50**, 12835 (1994).

[4] M. Eschrig and M.R. Norman, Phys. Rev. Lett. **85**, 3261 (2000).

[5] J. Carbotte, E. Schachinger, and D.N. Basov, Nature (London) **401**, 354 (1999).

[6] Ar. Abanov, A.V. Chubukov, and J. Schmalian, Adv. in Phys. **52**, 119 (2003).

[7] Ar. Abanov *et al.*, Phys. Rev. Lett. **89**, 177002 (2002).

[8] Ar. Abanov, A.V. Chubukov, and J. Schmalian, Journal of electron spectroscopy and related phenomena, v117, p129 (2001); A. Chubukov and M.R. Norman, Phys. Rev. B, **70**, 174505 (2004).

[9] H.Y. Kee, S.A. Kivelson, and G. Aeppli, Phys. Rev. Lett. **88**, 257002 (2002).

[10] Z.B. Huang, W. Hanke, E. Arrigoni, and D.J. Scalapino, Phys. Rev. B **68**, 220507(R) (2003).

[11] Z.B. Huang, W. Hanke, and E. Arrigoni, Europhys. Lett. **71** (6), pp.959 (2005).

[12] J.R. Schrieffer, J. Low Temp. Phys. **99**, 397 (1995).

[13] O.P. Sushkov and V. Kotov, Phys. Rev. B 70, 024503 (2004) and references therein.

[14] B.L. Altshuler, L.B. Ioffe, and A.J. Millis, Phys. Rev. B **52**, 5563 (1995).

[15] A.V. Chubukov, P. Monthoux, and D.K. Morr, Phys. Rev. B **56**, 7789 (1997).

[16] A.V. Chubukov and D.K. Morr, Physics Reports **288**, 355 (1997).

[17] R. Blankenbecler, D.J. Scalapino, and R.L. Sugar, Phys. Rev. D **24**, 2278 (1981).

[18] Note that in Ref. 12, the renormalization of Z was not included, i.e., the theoretical analysis assumed that $Z = 1$, and $\gamma = \Gamma$.

[19] In our convention, unbolded variables denote both Matsubara frequency and momentum, i. e., $p = (p_0, \mathbf{p})$ and $q = (q_0, \mathbf{q})$. We have set the frequencies to their minimum values, i. e., $p_0 = \pi T$ for fermions and $q_0 = 0$ for bosons.

[20] D. J. Scalapino, in *Superconductivity*, edited by R. D. Parks (Marcel Dekker, inc., New York, 1969), Vol. 1, Chap. 10,

pp. 449–560.

[21] S. R. White, D. J. Scalapino, R. L. Sugar, N. E. Bickers, and R. T. Scalettar, Phys. Rev. B **39**, 839 (1989).

[22] N. Bulut, D.J. Scalapino, and S.R. White, Phys. Rev. B **47**, 2742 (1993).

[23] C. Gröber, R. Eder, and W. Hanke, Phys. Rev. B **62**, 4336 (2000); R. Preuss, W. Hanke, C. Gröber, and H.G. Evertz, Phys. Rev. Lett. **79**, 1122 (1997).